

Chapter 3

Efficient Collection of ^{221}Fr into a Vapor Cell Magneto-optical Trap

3.1 Introduction

There has recently been considerable activity in the field of laser trapping of short-lived radioactive atoms. While a wide range of isotopes are being pursued, laser trapping of ^{21}Na [49], $^{37,38}\text{K}$ [54], ^{79}Rb [3], and $^{209,210,211}\text{Fr}$ [55] atoms has been experimentally realized. Efficient optical trapping is essential for creating large samples of rare atoms. Such samples are very appealing for tests of the standard model including atomic parity non-conservation (PNC), the electric dipole moment (EDM), and β decay [49]. Francium, which has no long-lived isotopes, is particularly interesting for these tests, because calculations predict PNC amplitudes and EDM enhancements to be 10 times larger in Fr than Cs [56, 57]. In this letter we demonstrate efficient trapping of ^{221}Fr . The general approach should work as well with any alkali isotope, and should make tests of the standard model possible in rare trapped atoms.

Various techniques have been developed to collect atoms into traps [7, 8], but since short-lived radioactive atoms are only available in limited quantities, improving the optical trap collection efficiency is a central issue. The highest efficiency yet demonstrated used a vapor cell magneto-optical trap (VCMOT) [15] in a glass cell coated with dryfilm. Using coated cells, Stephens *et al.* [30] and Guckert *et al.* [58] have demonstrated respectively 6% and 20% collection efficiencies of stable cesium. Similar techniques have been applied to trapping radioactive species of K, Rb, and Fr atoms [54, 3, 55], but with far lower trap efficiencies. We have created a highly efficient (56%) ^{221}Fr VCMOT in a coated cell and used it in spectroscopic measurements on ^{221}Fr .

A conventional VCMOT [15] traps a very small fraction of the available atoms. To obtain high collection efficiency, one must raise the collection rate and lower the vapor loss rate. The dependence and optimization of collection rate on various trap parameters has been previously investigated [32]. To have a high collection rate, a trap should have large, high-power laser beams. The trapping cell should be designed to maximize the ratio of the trap volume (region of laser beam overlap) to the cell surface area. To minimize the loss rate from the cell, the opening through which the radioactive atoms enter the cell must be small enough to minimize the leak rate, and the loss of atoms via adsorption to the glass walls must be significantly reduced. The latter is accomplished by coating the glass surfaces with dryfilm coatings made of silicon-based hydrocarbon polymers, which are then “cured” by exposure to alkali vapor. [31]

3.2 Theory

The analysis of the capture process differs from that of a conventional VCMOT. In a highly efficient VCMOT, the number of atoms in the vapor and the number of atoms in the trap are so strongly coupled that the vapor density cannot be considered constant. The time evolution of such a coupled system of N_t atoms in the trap and N_v atoms in the vapor depends on three rates: L, the loading rate of atoms from the vapor to the trap; C, the loss rate of atoms from the trap to the vapor due to collisions with background vapor atoms; and W, the loss rate of atoms from the vapor to the cell walls or out of the cell. In the case where a constant flux, I, of atoms enter the cell, the dependence can be described by two coupled differential equations:

$$\frac{d(N_t)}{dt} = -CN_t + LN_v,$$

$$\frac{d(N_v)}{dt} = CN_t - LN_v - WN_v + I.$$

The time evolution of the number of trapped atoms follows a double-exponential function,

$$N_t(t) = a_1 e^{-k_1 t} + a_2 e^{-k_2 t} + \frac{LI}{WC},$$

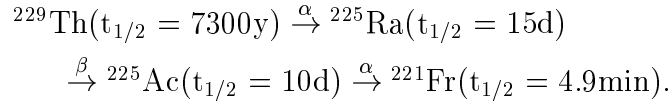
where $k_1 + k_2 = L + C + W$ and $k_1 k_2 = WC$. $N_t(t=0)$ and $N_v(t=0)$ fully determine a_1 and a_2 . We define trap efficiency (η) as the probability of trapping an atom that has entered the cell,¹

$$\eta = \frac{L}{(L + W)} = \frac{CN_t}{(CN_t + I)}.$$

3.3 Experimental Setup

3.3.1 Fr Source

The ^{221}Fr nuclei are produced in the decay chain



In order to produce a portable ^{221}Fr source with short-lived radioactivity, ^{225}Ac was first extracted out of a long-lived ^{229}Th sample, and deposited onto a small piece of platinum using one of two methods. Results reported here were obtained from a sample of ^{225}Ac chemically extracted from a ^{229}Th solution [59] and electroplated onto a Pt ribbon. In our preliminary measurements, we used ^{225}Ac implanted onto Pt via electrostatic collection [33]. The Pt ribbon was then placed in the cavity of an orthotropic oven [33] where ^{221}Fr daughters were continuously produced and distilled into a collimated

¹ Ref. [30] defines a recapture efficiency which is in general lower than η , but equal to η in the limit of a small collisional loss rate ($C \ll L, W$)

atomic beam. At the beginning of the experiment, the oven was loaded with $50 \mu\text{Ci}$ ^{225}Ac , which produced $2 \times 10^6 \text{ s}^{-1}$ of ^{221}Fr inside the oven. The full divergence angle of the atomic beam exiting the oven was measured to be 180 mrad. By counting the α particles from the decay of the ^{221}Fr , we measured a ^{221}Fr atomic beam flux of $3.8 \times 10^4 \text{ s}^{-1}$, or about 2% of the ^{221}Fr atom production rate inside the oven. Thirty days later, at the end of the experiment, the ^{221}Fr beam flux was $5.1 \times 10^3 \text{ s}^{-1}$, reflecting a decrease matching the natural decay of ^{225}Ac .

3.3.2 The Magneto-optical Trap

A schematic of the apparatus is shown in Fig. 3.1. Both the francium oven and the vapor cell were situated inside a chamber where the vacuum was maintained at 2×10^{-8} Torr even when the oven was heated to the operating temperature of 1050 °C. The cell was a quartz glass cube (4.4 cm inside dimension) whose top lid could be opened and closed via a mechanical feedthrough. Following the recipe developed by Stephens *et al.*[31], the cell walls were coated with a short-chain dryfilm called SC-77 (Silar Laboratories), and then cured by opening the cell lid and maintaining a Rb vapor in the cell at about 2×10^{-7} Torr for ten hours. The Fr atoms from the oven entered the cell through a 2 mm diameter hole at a lower edge of the cell. Over several days, the coating performance deteriorated, reducing the number of trapped Fr atoms by a factor of 3. This damage to the coatings could be attributed to heat or material evaporating from the oven, and was repaired by providing a continuous, low level curing with $\sim 1 \times 10^{-8}$ Torr of rubidium in the cell.

Up to 1W of light from a Ti:Sapphire ring laser was tuned to the D_2 line of Fr at 718 nm for trapping. The laser frequency was locked to the side of a Doppler-broadened I_2 absorption peak[60] that conveniently covered the frequency of the $7S_{1/2}$, $F=3 \rightarrow 7P_{3/2}$, $F=4$ cycling transition (Fig. 3.2). In addition, an SDL 100 mW diode laser at 817 nm was tuned to the D_1 line to pump atoms out of the $7S_{1/2}$, $F=2$ state. The frequency of the diode laser was tuned to the $7S_{1/2}$, $F=2 \rightarrow 7P_{1/2}$, $F=3$ transition and locked to a Fabry-Perot cavity, which was in turn actively stabilized to the rubidium D_2 line. This lock is described in detail in Appendix B.

3.3.3 Sensitive Detection

We assessed the performance of the wall coatings and found the correct laser frequencies by observing fluorescence from the room-temperature Fr vapor. We used an optical-optical double resonance technique to separate the fluorescence from light scattered off the cell walls. For this technique, a beam from the Ti:Sapphire laser was sent through the center of the cell, while its frequency scanned over one Doppler width (300 MHz) about the $7S_{1/2}$, $F=3 \rightarrow 7P_{3/2}$, $F=4$ cycling transition. A 60 mW beam from the 817 nm diode laser, chopped at 100 Hz, co-propagated and overlapped the Ti:Sapphire beam through the cell. The diode laser frequency was tuned close to the $7S_{1/2}$, $F=2 \rightarrow 7P_{1/2}$, $F=3$ transition to pump atoms from the $7S_{1/2}$, $F=2$ to the $7S_{1/2}$, $F=3$ state. The population of the $7S_{1/2}$, $F=3$ state was therefore fully modulated for

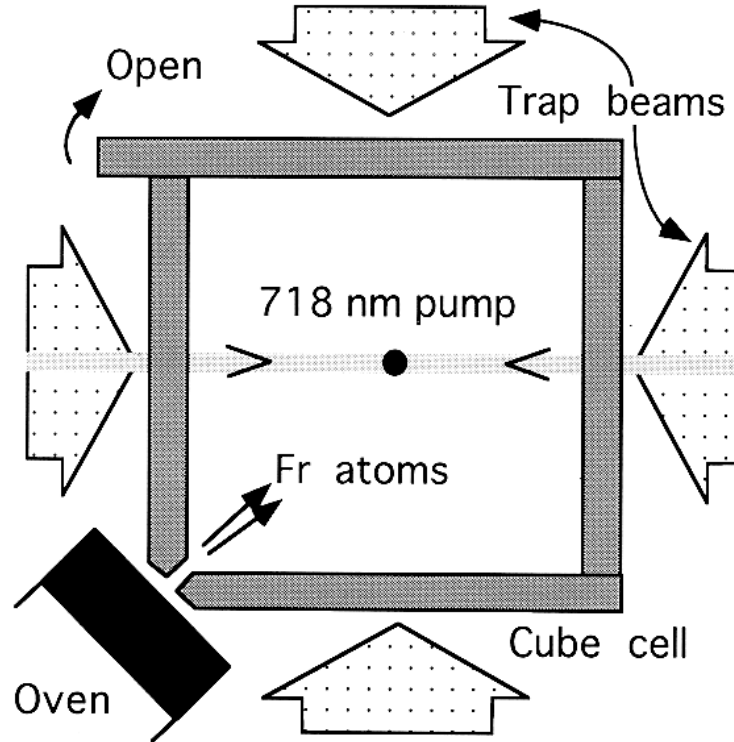


Figure 3.1: A diagram of the ^{221}Fr trap setup. Both the oven and the cell were situated inside a vacuum chamber with 10 cm diameter windows. The same oven and cell assembly was used for the ^{221}Fr vapor fluorescence measurements.

the group of atoms in resonance with both laser beams. Because this was a narrow velocity group, the resulting resonance feature was sub-Doppler (50 MHz FWHM). The resulting modulated fluorescence at 718 nm generated near the center of the cell was imaged onto a low noise photo-diode through a 718 nm interference filter and demodulated with a lock-in amplifier. Thus we were capable of detecting as few as 600 atoms in the entire cell, or equivalently 1 Fr atom in resonance in the viewing region, with a signal to noise ratio (SNR) of $1/\sqrt{s}$. By monitoring the exponential buildup of the number after the cell lid was closed, we determined the loss rate of Fr atoms from the vapor (W) to be $1.59(9) \text{ s}^{-1}$, and a constant flux of $2.3 \times 10^3 \text{ s}^{-1}$ Fr atoms entering the cell.

We then trapped the Fr atoms in a VCMOT using 4 cm diameter laser beams. These beams provided a six-beam-total intensity of up to 110 mW/cm^2 in the cell. In addition, a 60 mW, 4 cm diameter beam from the diode laser at 817 nm was sent through the cell four times along two normal axes of the cube cell. A set of anti-Helmholtz coils generated the MOT quadrupole field gradient of $\sim 7 \text{ Gauss/cm}$.

The laser light scattered from the six cell walls made detection of the 718 nm fluorescence from the trapped Fr atoms impossible. Instead, to further avoid scattered light and thereby increase our sensitivity, we imaged the 817 nm repump fluorescence

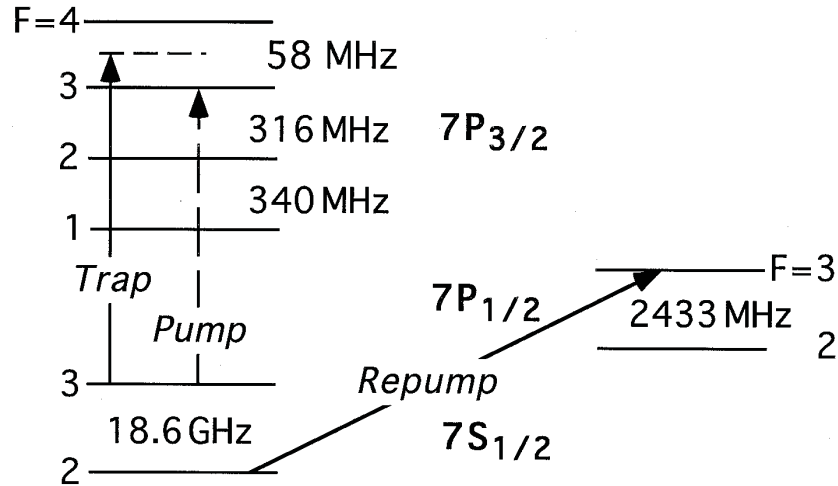


Figure 3.2: The atomic level diagram of ^{221}Fr . In our ^{221}Fr trap, the trap laser (718 nm) was tuned to ~ 30 MHz below the $7S_{1/2}$, $F=3 \rightarrow 7P_{3/2}$, $F=4$ cycling transition, and the repump laser (817 nm) was tuned to the $7S_{1/2}$, $F=2 \rightarrow 7P_{1/2}$, $F=3$ transition. To detect the trapped atoms, a 718 nm pump beam (2 mm diameter, 50 mW/cm^2), tuned to the $7S_{1/2}$, $F=3 \rightarrow 7P_{3/2}$, $F=3$ transition, was chopped to modulate the 817 nm fluorescence from the trap.

from the trapped atoms onto a photodetector. This light was observed through a cell window not illuminated by any repump beams and through a 817 nm bandpass interference filter. The 817 nm fluorescence was modulated using a small, frequency-shifted 718 nm pump beam that was chopped and retro-reflected through the trap center (see Fig. 3.1). This beam increased the fractional population in the $7S_{1/2}$, $F=2$ state to 70% without affecting the trap loading rate. This detection scheme allowed us to detect as few as 15 trapped Fr atoms with a SNR of $1/\sqrt{s}$ in the presence of large amounts of scattered light. The trap contained an estimated 900 atoms, but this is a lower limit assuming that both the 718 nm pump and the repump lasers were tuned to resonance. This trapped atom sample could be maintained for many hours.

3.4 Results

3.4.1 Trapping Efficiency

Figure 3.3 shows a trap loading curve fitted to the double-exponential function predicted by our model. The fit gives the trap rate constants, from which we calculate the trapping efficiency to be $\eta = \frac{L}{(L+W)} = 56(10)\%$. As a check, $\eta = \frac{CN_t}{(CN_t+I)}$ gives a lower limit of 30% assuming the repump laser is tuned to resonance, but can be as high as 50% when plausible detunings are assumed in calculating N_t . The atomic fluxes at various stages of the experiment are listed in Table 3.2, showing a total efficiency of 0.4% from production to trapping. Engineering improvements in the oven and in the

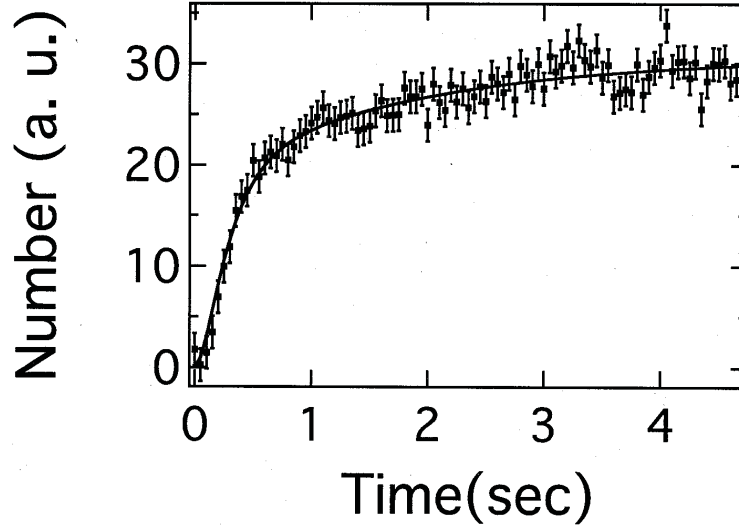


Figure 3.3: The number of atoms (in arbitrary units) loaded into a ^{221}Fr trap vs. time. In a trap with a high collection efficiency, the loading signal is expected to be a double-exponential function. Because the signal was filtered by a low-pass network with a time constant $\tau = 100$ ms, it was fitted with the function $b_1[1-\exp(-k_1t)] + b_2[1-\exp(-k_2 t)] - \tau[b_1k_1 + b_2k_2][1 - \exp(-t/\tau)]$. The best fitting results were $k_1 = 4.8(1.0) \text{ s}^{-1}$ and $k_2 = 0.57(23) \text{ s}^{-1}$. Combining these rates with the measured result that on average a Fr atom stayed in the vapor for $1/W = 0.63(4) \text{ s}$, we derived that, on average, a Fr atom stayed in the trap for $1/C = 0.58(27) \text{ s}$ and it takes $1/L = 0.48(19) \text{ s}$ to load a Fr atom from the vapor into the trap. These rates are consistent with those found in Rb traps, and imply a trap efficiency of $L/(L+W) = 56(10)\%$.

coupling into the cell would significantly improve the total efficiency. An orthotropic source has operated with a 15% efficiency, and 50% (limited by diffusion of Fr into the oven walls) is theoretically possible[33].

3.4.2 Spectroscopy

We have made spectroscopic measurements on ^{221}Fr using our apparatus. In the thermal vapor, we measured the hyperfine splittings of the $7P_{3/2}$ and $7P_{1/2}$ levels. We observed the individual hyperfine transitions by scanning the 718 nm laser, while the 817 nm diode laser was set (to either the $F=2 \rightarrow F'=3$ or $F=2 \rightarrow F'=2$ transition) to select one velocity group of atoms. We obtained the splittings by measuring the frequency differences between each hyperfine line (Table 3.1) using a high-resolution λ -meter[61]. By checking against known splittings and wavelengths in rubidium, we found the accuracy of the λ -meter to be 3 MHz or less when measuring small differences, but 50 MHz when measuring absolute frequency. This is because uncertainties in the refractive index of air and laser beam alignment are largely canceled in a frequency difference measurement.

Table 3.1: Various rates, fluxes, and efficiencies on Dec. 17-18, when the source strength was 9 μCi . Total efficiency is 0.4%. Data in row (4) are deduced from flux entering cell and trap efficiency.

| | Stage | ^{221}Fr Flux (s^{-1}) | Efficiency |
|-----|---------------------|--|------------|
| (1) | Produced in oven | 3.3×10^5 | |
| (2) | Exit oven | 7×10^3 | 2% of (1) |
| (3) | Enter cell | 2.3×10^3 | 33% of (2) |
| (4) | Collected into trap | 1.3×10^3 | 56% of (3) |

Using the trapped atoms as a frequency reference, we have measured the wavenumbers of the D_1 and D_2 transitions of ^{221}Fr (Table 3.1). While the wavenumber of the D_1 transition measured here is in agreement with the number measured by the ISOLDE collaboration[62, 63], our value of the D_2 transition is lower by $3 \sigma_{STD}$. As a check on our calibration, we measured the wavenumber of the I_2 line that is only 0.5 GHz away from the D_2 trapping transition and found an excellent agreement (difference = $1(3) \times 10^{-3} \text{ cm}^{-1}$) with the I_2 atlas[60].

3.5 Conclusions

We have demonstrated and analyzed the dynamics of highly efficient collection of short-lived radioactive alkali atoms in an optical trap. The techniques used here, including the optimized VCMOT, the orthotropic source, and sensitive detection, can be easily applied to other alkalis as well ² Future applications will likely employ immediate, efficient transfer of trapped atoms out of the cell into a much longer-lived trap (see, for example, Refs. [18, 24, 64] and Chapter 2. By combining a stronger and currently available ^{221}Fr source (flux $\sim 10^6/\text{s}$) with a double-MOT system (trap lifetime $\sim 10^2$ s), a sample of 10^8 trapped ^{221}Fr atoms could be prepared for the next generation of

² Most alkalis would be easier than ^{221}Fr , which has an unusually small excited state splitting combined with a large ground state splitting.

Table 3.2: The hyperfine constants and wavenumbers of ^{221}Fr . The wavenumbers of the previous work were derived from the published wavenumbers of ^{212}Fr and isotope shifts [17].

| | ISOLDE [62, 63] | Current Work |
|-------------------------------------|-----------------|----------------|
| A ($7P_{3/2}$) MHz | 65.4(2.9) | 66.5(0.9) |
| B ($7P_{3/2}$) MHz | -259(16) | -260.0(4.8) |
| A ($7P_{1/2}$) MHz | 808(12) | 811.0(1.3) |
| σ (D_1) cm^{-1} | 12236.6601(20) | 12236.6579(17) |
| σ (D_2) cm^{-1} | 13923.2118(20) | 13923.2041(17) |

high precision spectroscopy measurements to test fundamental symmetries.